International Journal of GEOMATE, Jan., 2026 Vol.30, Issue 137, pp.99-106
ISSN: 2186-2982 (P), 2186-2990 (O), Japan, DOI: https://doi.org/10.21660/2026.137.g15223
Geotechnique, Construction Materials and Environment

DEVELOPMENT OF A HAZARD ASSESSMENT APPROACH BASED ON AN INTEGRATED MODEL FOR LARGE WOODY DEBRIS DISCHARGE IN DAM WATERSHEDS

Yunhao Liu[1], Daisuke Komori[1,2, 3], Sartsin Phakdimek[4] and Yuta Abe[5]

[1]Graduate School of Environmental Studies, Tohoku University, Japan;
[2] Green Goals Initiative, Tohoku University, Japan;
[3] International Research Institute of Disaster Science, Tohoku University, Japan;
[4] School of Geotechnology, Institute of Engineering, Suranaree University of Technology, Thailand;
[5] Department of Civil and Environmental Engineering, Tohoku University, Japan

*Corresponding Author, Received: 30 May 2025, Revised: 29 Nov. 2025, Accepted: 05 Dec. 2025

ABSTRACT: This study proposes a physically based framework for assessing the hazard of large woody debris (LWD) discharge in dam watersheds under extreme rainfall conditions. The method integrates rainfall return-level analysis, landslide-induced LWD recruitment modeling, and discharge simulation using a double storage function with the lumped hydrological method at a watershed scale. It was applied to five representative dam watersheds in Japan to simulate the potential minimum, maximum, and expected LWD discharge volumes under varying rainfall return periods. The results demonstrate that the framework effectively captures the variability in discharge responses across sites and identifies dam-specific rainfall thresholds for potential LWD discharge. Particularly, the use of expected initial storage conditions significantly improves the reliability of hazard estimation. The observed LWD discharge records were consistently bound by the simulated discharge ranges, validating the model's applicability. In contrast to traditional observation-based approaches, this framework enables estimation of low-frequency hazards. It offers a practical tool for risk-informed reservoir management and indicates the importance of integrating physical processes in LWD hazard prediction. These findings contribute to understanding inter-site differences in LWD storage and transport behavior, enabling more proactive hazard mitigation planning under increasing extreme weather events.

Keywords: Large woody debris, Landslide, Recruitment, Storage, Hazard assessment

1. INTRODUCTION

Large woody debris (LWD) refers to woody material (fallen trees, logs, large branches, etc.) within river channels, typically defined by pieces over ~0.1 m in diameter and 1 m in length [1]. In steep and forested basins, LWD is primarily recruited from hillslope failures (landslides, debris flows) and riverbank erosion during intense storms [2]. LWD in river channels has become a focus of increasing scientific interest, being regarded as a functional component of fluvial ecosystems, as important as sediment and riparian vegetation [3,4].

However, when extreme rainfall or flood events occur, mobilized LWD can cause severe hazards: LWD transported by floods often accumulate into logjams that block bridge openings or dam spillways, exacerbating upstream flooding and even causing structural failures [5]. Globally, numerous flood disasters have been aggravated by LWD transport. For example, a catastrophic flash flood in Italy (October 2011) delivered ~540 mm of rain in 8 hours, generating abundant driftwood that clogged numerous bridges and led to severe damage and loss of life [6]. In monsoon- and typhoon-prone mountain regions such as Thailand and Japan, landslides and related hydrogeomorphic hazards can mobilize large wood that is subsequently routed downstream within debris flows and floodwaters, posing serious risks to communities and infrastructure. In Thailand, this hazard cascade is exemplified by the 2001 debris flow–flood disaster in the Nam Ko area, Phetchabun Province, and by LWD accumulations at check dams and reservoirs that have aggravated flood impacts [7]. Similar processes have been documented in Japan, where typhoon-triggered landslides during Typhoon Lionrock in Iwate Prefecture and the geotechnical damage in Miyagi Prefecture caused by Typhoon Hagibis illustrate the high vulnerability of settlements to LWD-entraining flows [8,9]. This prevalence of LWD-induced damage in these areas underlines the urgent need to better understand LWD dynamics and mitigate its hazards in such environments.

Recent studies have quantified LWD discharge at many reservoir dams, validating model predictions against measured outflows. For example, a watershed-scale LWD integrated model has been applied to 212 dam reservoirs across Japan, successfully reproducing annual LWD export volumes in 134 basins (≈63%) [10]. This model builds on earlier work in which a double-storage function framework was calibrated on 20-year records at five reservoirs in northeast Japan [11]. In that initial study, the model achieved Nash–Sutcliffe

efficiencies ≥0.7 in 4 of 5 basins, indicating high fidelity to observed LWD discharge [12]. The analysis revealed that LWD discharge is governed by two key processes: (1) direct discharge of newly recruited LWD during rainfall-induced shallow landslides, and (2) a slower "baseflow" discharge of older LWD previously stored on slopes or in channels. In other words, landslide-induced LWD recruitment produces short-lived peaks in LWD discharge, whereas substantial volumes of legacy LWD remain temporarily stored on hillslopes and in channels and are released gradually during subsequent flow events. These studies emphasize that accurately capturing this storage and transport processes are essential for understanding LWD dynamics.

In contrast, widely used LWD models have tended to focus on estimating event-scale export rather than representing the full sequence from recruitment and storage to downstream discharge [13,14]. Logistic landslide models combined with forest cover data, for example, can reproduce LWD volumes generated by rainfall-induced landslides at the scale of reservoirs or river reaches, but they usually treated discharged LWD as newly mobilized material from that event and didn't track how LWD is stored and remobilized in watershed. This limitation is reinforced by the scarcity of repeated measurements of LWD volume on hillslopes and in channels, which makes it difficult to document changes in storage and to evaluate models over decadal time scales. A different line of research has developed long-term mass-balance frameworks that explicitly include LWD storage by representing in-stream wood as a lumped reservoir with simple decay or discharge rules and by simulating LWD budgets over decades to centuries [15,16]. These models derive general relationships between recruitment, storage, and discharge, but they remain highly idealized because they are only weakly linked to actual rainfall conditions. Therefore, existing approaches either capture event-scale LWD generation without resolving long-term storage dynamics, or they treat storage in a simplified way without explicitly representing how different rainfall intensities drive magnitude of LWD recruitment and discharge.

In response to these gaps, this study develops a hazard assessment framework based on an integrated LWD discharge model [11]. The framework combines extreme-rainfall frequency analysis with a rainfall-induced landslide recruitment module and a double-storage function for LWD transport at the watershed scale, allowing annual LWD discharge to be simulated under a range of design rainfall scenarios. It is applied to five representative dam watersheds in central and northeastern Japan to estimate the minimum rainfall return period at which LWD discharge is likely to begin and to quantify the minimum, maximum and expected discharge volumes associated with different return levels. By explicitly accounting for LWD storage and gradual release together with variability in recruitment, the approach links the amount of LWD supplied by landslides to the volume that can be discharged to reservoirs during rare, high-magnitude events. In doing so, it extends previous observation-based and event-scale models into a practical tool for risk-informed reservoir management and for interpreting site-specific differences in LWD discharge behavior under Japan's various rainfall conditions.

2. RESEARCH SIGNIFICANCE

This study presents a novel, physically based framework for assessing large woody debris (LWD) discharge hazards under extreme rainfall. It uniquely integrates rainfall return-level analysis, landslide-driven recruitment, and storage–transport dynamics using an adapted LWD discharge model within a unified budget approach. Unlike conventional observation-based methods, the framework estimates low-frequency and site-specific hazards by simulating minimum, maximum, and expected discharge volumes under various rainfall scenarios. Its incorporation of expected initial storage conditions enhances prediction reliability, offering an innovative tool for proactive reservoir management amid increasing extreme weather events.

3. STUDY SITES

Five dam watersheds were selected as study sites for this research, located across six prefectures in central and northeastern Japan: Nagano, Niigata, Tochigi, Yamagata, Akita, and Iwate. These watersheds were chosen to represent a range of topographic and climatic conditions characteristic of mountainous regions prone to rainfall-induced landslides and LWD transport. The spatial distribution of Dam No. 1 to No. 5 is illustrated in Fig.1. Their key physical characteristics are summarized in Table 1.

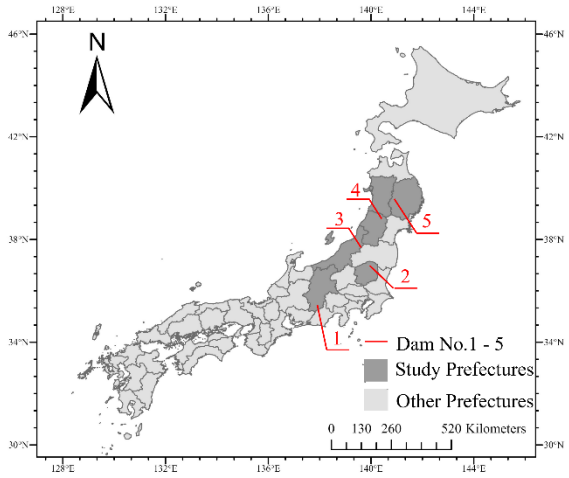

Fig.1 Locations of the five selected dam watersheds

Table 1 Basic characteristics of the five selected dam watersheds

No.	Dam	Area (km^2)	Length (km)
1	Katagiri	14.86	8.58
2	Shiobara	123.96	113.29
3	Tainaikawa	72.68	55.44
4	Kamuro	22.29	15.23
5	Yuda	577.49	512.25

Note: Area refers to total watershed area; length refers to total river length within the watershed.

Given the temporal coverage and spatial variability of the selected sites, this discharge data reflects a wide range of hydrological and geomorphic conditions relevant to LWD transport.

In Japan, local reservoir management agencies monitor the total annual volume of LWD transported into reservoirs [11]. The highest single-year LWD discharge volume and the associated annual maximum 24-hour rainfall for each study dam during the period 1996–2021 are summarized in Table 2.

Table 2 Highest single-year LWD discharge volumes and associated annual maximum 24-hour rainfall for each study dam (1996–2021).

No.	Max. Volume (m³)	Max. Rainfall (mm/24hrs)
1	610	288
2	3295	343
3	397	281
4	246	242
5	2490	240

Note: Dam No. 1–5 correspond to the five study dams listed in Table 1. Max Volume indicates the highest recorded annual LWD discharge for each dam during 1996–2021. Max Rainfall refers to the maximum 24-hour rainfall over the corresponding watershed in the same year.

It reflects LWD responses to extreme rainfall events, as represented by the years of maximum discharge. Despite the limited range of 24-hour rainfall (240–343 mm), it corresponds to varying rainfall intensities across sites (e.g., different return periods), which will be examined in this study.

4. METHODS

The objectives of this study are two parts: (1) identify the minimum rainfall return period at which potential LWD discharge begins at each site, and (2) quantify the range of potential LWD discharge (including minimum, maximum, and expected values) under various return periods. In addition, the threshold rainfall return period and corresponding return level at which LWD discharge begins will be identified. The overall framework and methodology are presented in this section.

4.1 Rainfall Return Period and Level Analysis

Annual maximum 24-hour rainfall data (1996–2021) within five dam watersheds were extracted from the Radar-AMeDAS dataset provided by the Japan Meteorological Agency, with a spatial resolution of 1 km. For each dam watershed, the series of annual maximum was fitted to the Generalized Extreme Value (GEV) distribution to estimate rainfall intensities corresponding to different return periods [12]. The GEV distribution is widely used for hydrological hazard assessment and is defined as:

$$F(x) = \exp\left\{-[1+\xi(\frac{x-\mu}{\sigma})]^{-1/\xi}\right\} \quad (1)$$

where μ, σ, and ξ are the location, scale, and shape parameters, respectively. Parameters were estimated using the L-moments method, based on 26 years (1996–2021) of rainfall data.

From the fitted distribution, the rainfall return levels x_T within in each dam watershed were derived using the inverse of Eq. (1), expressed as:

$$x_T = \mu + \frac{\sigma}{\xi}\left[(-\log(1-\frac{1}{T}))^{-\xi} - 1\right] \quad (2)$$

Return levels for various return periods T (e.g., 3–200 years) were calculated and used as rainfall inputs for subsequent landslide modeling under different hazard scenarios. These synthetic extreme rainfall values allow comparison between observed historical conditions and potential future extremes.

4.2 LWD Recruitment Simulation

In this study, the model was applied to five dam watersheds in Japan using two types of rainfall input: (1) observed annual maximum 24-hour rainfall for the monitoring period and (2) design rainfall return levels derived in the previous section. For each watershed, this generated two parallel sets of outputs: annual LWD recruitment volumes driven by historical annual maximum 24-hour rainfall, and potential recruitment volumes associated with specified return periods. LWD recruitment from shallow landslides was computed with a physical, rainfall-induced landslide model operating on a 30 m grid, in which cells with a factor of safety less than 1.0 were treated as unstable. Within these unstable areas, tree density and an assumed per-piece wood volume were used to convert failure area intersecting the active channel zone into recruited LWD volume, which was then aggregated to the watershed scale for each year. These recruitment estimates were used as inputs to the LWD discharge simulation framework described in the next section.

4.3 Discharge Simulation and Hazard Assessment

The discharge of LWD from dam watersheds was simulated using a double storage function model based on the lumped hydrological method, following the approach of [10,11]. This section describes how the proposed model is used to calculate the expected, maximum, and minimum potential LWD discharge.

This section involved three steps. In the first step, dam-specific model parameters for each study site were identified by fitting the model to observe annual LWD discharge records from 1996 to 2021. For each dam, annual recruitment volumes were used as inputs, and parameter sets were determined by maximizing the Nash–Sutcliffe Efficiency (NSE) between observed and simulated discharge values [17]. The structure of the model remained fixed, and parameter optimization was conducted independently for each dam watershed. The structure of the model and its key parameters are illustrated in Fig. 2.

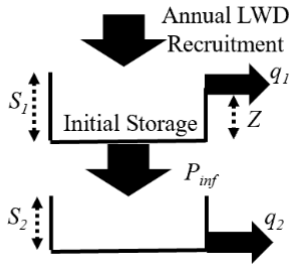

Fig.2 Conceptual framework of the double storage function model

Where S_1 and S_2 are storage volumes in first and second tank (m^3), respectively. Z is the capacity of the first tank, which is one of the model parameters determined by NSE method. Sum of q_1 and q_2 is the annual LWD discharge volume (m^3). The governing equations and parameter definitions are presented below. When $S_1 \geq Z$:

$$q_1 = S_1(n) - Z \tag{3}$$

When $S_1 < Z$:

$$q_1 = 0 \tag{4}$$

$$P_{\inf} = b \cdot S_1(n) \tag{5}$$

$$S_1(n+1) = S_1(n) + P - P_{\inf}(n) \tag{6}$$

$$\frac{dS_2}{dt} = P_{\inf} - q_2(n) \tag{7}$$

$$S_2 = k \cdot q_2^p \tag{8}$$

where b, k and p are parameters, n is time (in years). The following equation defines the NSE:

$$\text{NSE}=1-\frac{\sum_{m=1}^{N}(q_{obs}(m)-q_{sim}(m))^2}{\sum_{m=1}^{N}(q_{obs}(m)-q_{ave}(m))^2} \tag{9}$$

where N is the simulation period (year), m is a year from 1 to N, q_{obs} is the annual observed LWD discharge volume(m^3), q_{sim} is the annual simulated LWD volume (m^3), q_{ave} is the average annual observed LWD volume (m^3).

Subsequently, 10,000 annual LWD recruitment values were randomly generated for each study site. The model was run for each random value using the estimated parameters from the first step, and the resulting storage-to-capacity ratios in first tank were recorded. These ratios were then used to compute an expected initial storage-to-capacity ratios ($r= S_1/Z$) via a weighted average approach, representing the actual LWD storage conditions within dam watershed, which enables the estimation of expected potential LWD discharge. The framework for calculating the expected storage percentage is illustrated in Fig. 3.

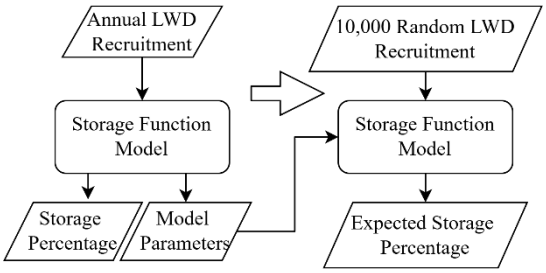

Fig.3 Schematic diagram of expected storage percentage calculation

Finally, using LWD recruitment volumes estimated under return-level rainfall conditions (mm/24 hrs), the double storage function model was run under three initial storage scenarios: empty (0%), saturated (100%), and the expected storage percentage. For each dam watershed and return period, the model produced a distribution of annual LWD discharge volumes, from which the minimum, maximum, and expected values (in m^3/year) were derived. These results enabled comparative hazard assessments across sites under varying rainfall conditions.

5. RESULTS AND DISCUSSIONS

5.1 Model Parameters Estimation

The double storage function model described above was applied to five dam watersheds using observed annual maximum 24 hours rainfall and LWD discharge records from 1996 to 2021. Model

parameters were determined independently for each site, and the simulated annual LWD discharge was compared with observations to evaluate performance by NSE. The model parameters determined by the NSE are summarized in Table 3.

Table 3 Model Parameters and NSE for each study site

No.	*Z*	*b*	*k*	*p*	NSE values
1	12,000	0.11	0.0001	100	0.900
2	14000	0.215	0.0476	2.44	0.807
3	89,000	0.17	0.0001	100	0.462
4	8,500	0.005	0.0051	9.10	0.408
5	9,000	0.47	0.0001	100	0.705

Note: Dam No. 1–5 correspond to the five study dams listed in Table 1. Z,b,k and p are model parameters in double storage function model

The calibrated parameter sets show pronounced contrasts among the five dam watersheds (Table 3). The storage capacity (Z) spans from 8,500 m³ at Kamuro (No. 4) to 89,000 m³ at Tainaikawa (No. 3), whereas Katagiri, Shiobara and Yuda have intermediate values of 9,000–14,000 m³. This indicates that the first tank in the Tainaikawa model can accommodate a much larger LWD volume before overflow, while Kamuro is represented as having relatively limited upstream storage. The transfer coefficient (b) also varies widely, from 0.005 at Kamuro to 0.47 at Yuda, suggesting strong differences in the proportion of recruited LWD that is routed from the first to the second tank. In addition, the second-tank parameters (k) and (p) form two distinct groups: three basins (Katagiri, Tainaikawa and Yuda) share a very large (p) combined with a small (k), whereas Shiobara and Kamuro have smaller (p) and larger (k). Given the formulation ($q_2 = k \times S_2^p$), this implies that in the former group the second-tank discharge becomes highly sensitive to large storage, while in the latter group it increases more gradually with (S_2).

Model performance, as measured by the Nash–Sutcliffe efficiency, ranges from about 0.4 to 0.9 across the five sites. Katagiri (No. 1) and Shiobara (No. 2) exhibit the highest NSE values (0.90 and 0.81), indicating that the model reproduces their annual variability in LWD discharge relatively well, whereas Kamuro (No. 4) and Tainaikawa (No. 3) show only lower accuracy, and Yuda (No. 5) lies in between. No single parameter alone explains these differences, but the lowest NSE values occur at sites with either an extremely large (Z) (Tainaikawa) or a very small (b) (Kamuro), suggesting that the present double-storage structure has difficulty capturing their actual storage–release behavior with a single parameter set. This highlights that parameter identifiability may differ among basins, even when the same model structure is used.

A comparison of Tables 1 and 3 further shows that watershed area and river length do not directly control the optimized storage capacity. Tainaikawa, which has an intermediate watershed area and river length, attains by far the largest Z, whereas Yuda, the largest basin in terms of both area and channel length, has only a modest first-tank capacity of 9,000 m³. If storage capacity is qualitatively normalized by watershed area, Tainaikawa therefore has a much larger effective LWD storage capacity per unit area than the other catchments, while Yuda has the smallest. This pattern indicates that the calibrated parameters reflect not only simple geometric descriptors, but also other site-specific factors such as channel network configuration, valley confinement and long-term LWD supply that are not explicitly represented in the model. Therefore, the results support the need for site-specific parameter estimation rather than transferring parameter values solely based on watershed size.

5.2 Expected Initial Storage Estimation

The expected initial storage-to-capacity ratios ($r = S_1/Z$) for the five dam watersheds, estimated through 10,000 stochastic simulations per site, are spatially presented in Fig. 5.

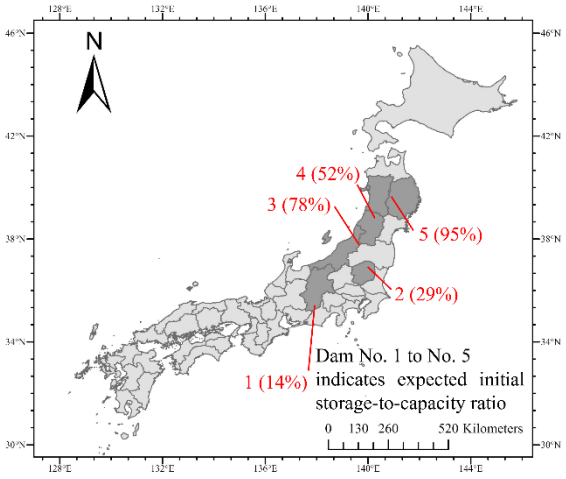

Fig.5 Spatial distribution of expected storage-to-capacity ratios (r) at five study dams.

The values vary substantially among sites, ranging from 14% at Katagiri Dam to 95% at Yuda Dam. Katagiri and Shiobara Dams exhibited relatively low expected storage ratios (14% and 29%, respectively), indicating that annual LWD recruitment volumes at these sites were generally insufficient to saturate the LWD storage capcacity within in watershed. In contrast, Yuda Dam showed a markedly high value of 95%, indicating a high

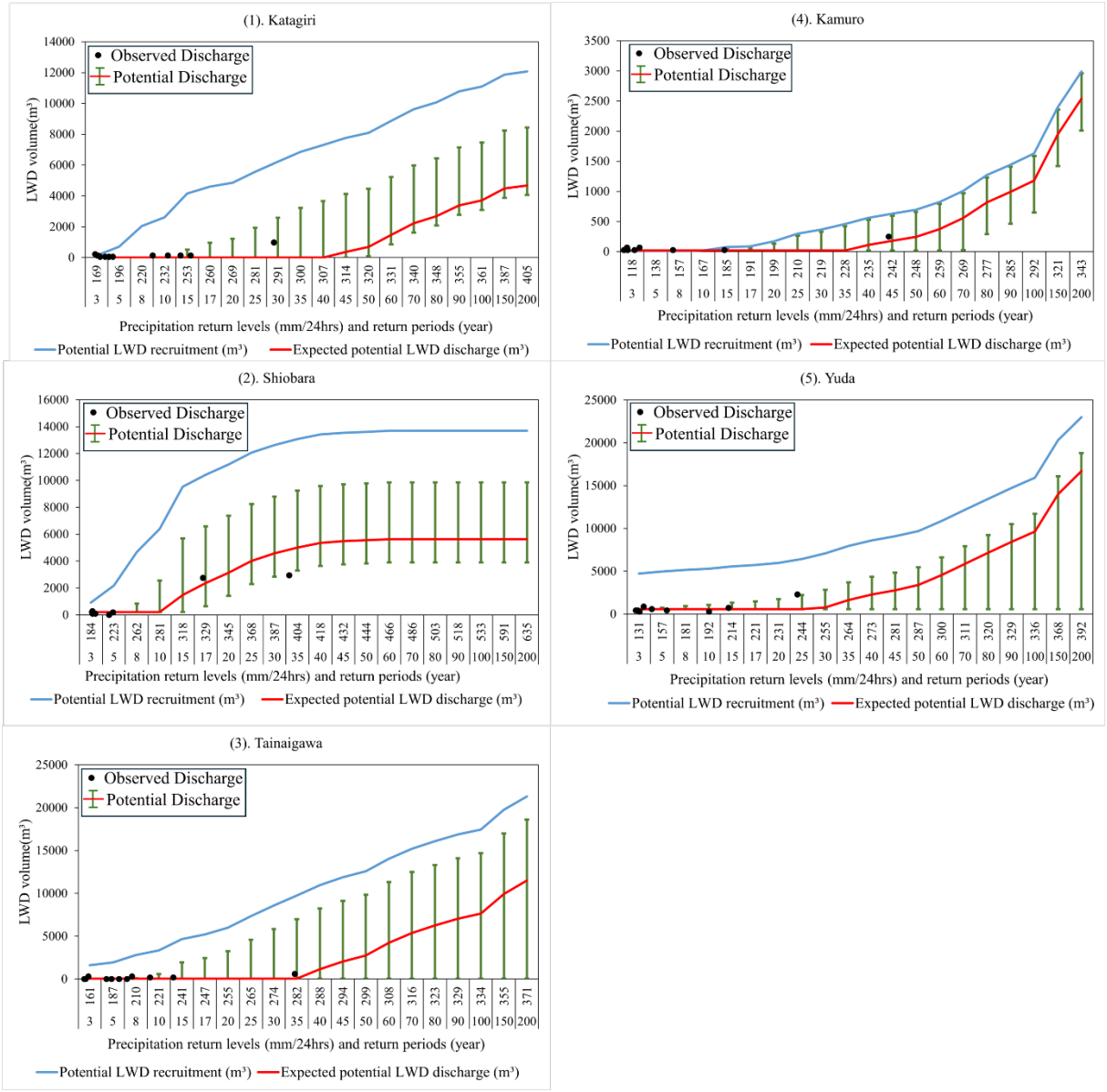

Fig.6 Simulated hazard assessment of potential LWD discharge volume under varying rainfall return periods for the five study sites.

possibility of storage capacity exceedance. Tainaikawa and Kamuro Dams showed intermediate ratios of 78% and 52%, respectively. These differences reflect variation in modeled LWD accumulation dynamics across the study of watersheds under historical discharge conditions.

5.3 Hazard Assessment Results

The results of LWD discharge simulations under rainfall return-level scenarios are presented in Fig. 6, which illustrates the estimated potential minimum, maximum, and expected discharge volumes for the five study sites. Horizontal axes represent rainfall return periods T (e.g., 3–200 years) and corresponding to different return levels (mm/24hrs), and vertical axes show LWD volumes (m³/year), including simulated potential discharges (q_{min},q_{exp} *and* q_{max}), model input potential recruitment (P), and observed records (q_{obs}). The black dots showed the selected LWD discharge records. As shown in Fig. 6, all black dots representing observed LWD discharge volumes fall within the modeled range of potential discharge, indicating the reliability of the hazard assessment results. Although the observational records are primarily corresponded to return periods shorter than 45 years (e.g., Fig. 6(4)), the modeling framework developed in this study enables estimation of LWD discharge for lower-frequency events beyond the observed range. This represents a significant improvement over approaches that rely exclusively on historical records, which are

inherently limited in their ability to assess rare but potentially large volume LWD discharge events.

5.3.1 Return period and potential LWD discharge

One notable feature in Fig. 6 is the substantial variation in rainfall return levels across all sites within the same return periods. This disparity is particularly critical when determining the minimum rainfall return period at which LWD discharge is likely to occur.

Among the five study sites, the Shiobara and Katagiri dam watersheds were selected representative cases to illustrate the contrasting responses of LWD discharge to varying rainfall return periods within each watershed.

Shiobara Dam (Fig. 6(2)) showed a rapid increase in expected discharge volume (q_{exp}) starting at a return period of 10 years (281 mm/24hrs), with q_{exp} reaching 217 m³ and q_{max} exceeding 2500 m³.

In contrast, Katagiri Dam (Fig. 6(1)) exhibited a more gradual discharge response. q_{exp} began to increase noticeably only after a 40-year return period (307 mm), reaching 4681 m³ at 200 years (405 mm), while q_{max} peaked at 8430 m³. The findings suggest that the response of LWD discharge to rainfall return periods and levels varied significantly among different dam catchments.

The remaining three catchments fall between these two and illustrate additional response types. At Kamuro and Yuda Dams, the expected discharge begins to rise at relatively short return periods, but the increase remains moderate until rainfall exceeds intermediate thresholds, after which both q_{exp} and q_{max} grow rapidly. Tainaikawa exhibits a contrasting pattern, with little response at short return periods but a very steep increase in discharge once the threshold is exceeded, reflecting its large, calibrated storage capacity (Z) and high recruitment potential. In summary, these contrasting response curves suggest that watersheds can be broadly grouped into low-threshold, high-sensitivity systems and high-threshold, delayed-response systems, with important implications for how often hazardous LWD discharges are likely to occur under a given regional rainfall pattern.

5.3.2 LWD storage characteristics of dam watershed

The results can be used to further explore LWD discharge risks from a storage characteristics perspective, based on their contrasting proportions of discharge to recruitment volume. These ratios reflect the overall capacity of each watershed to retain LWD before it is discharged, offering an additional dimension to hazard assessment. The values for catchments No.1 to No.5 were 0.62, 0.68, 0.80, 0.96, and 0.62, respectively.

Among all sites, Kamuro Dam exhibited a q_{max} to P ratio of 0.96, placing it among the highest. This suggests that under extreme rainfall, nearly the entire volume of recruited LWD may be discharged downstream. Such a condition indicates weak long-term storage capacity and frequent saturation of LWD retention potential, increasing the likelihood of high-magnitude discharge events even under relatively moderate recurrence intervals.

In contrast, Katagiri Dam and Yuda Dam showed the lowest discharge-to-recruitment ratios among the five sites, with values of 0.62 for q_{max}. These results reflect comparatively strong LWD storage performance, where most of the recruited LWD is retained within the watershed. Consequently, the probability of sudden large-scale LWD discharge events is reduced, making this site relatively low risk from a storage-based hazard perspective.

6. CONCLUSIONS

This study estimated the potential discharge of large woody debris (LWD) in five dam watersheds under varying rainfall return periods, focusing on the minimum, maximum, and expected annual discharge volumes. By incorporating stochastic recruitment and evaluating discharge ranges under different storage scenarios, the expected potential discharge was successfully simulated. Simulation results revealed clear inter-watershed differences in discharge behavior and storage characteristics, with expected discharge values serving as a reliable indicator of site-specific LWD discharge risk. To further enhance the generalizability of the proposed hazard assessment framework, future studies are encouraged to include a broader range of dam watersheds with diverse geomorphological and climatic conditions. Expanding the number of study sites would enable a more comprehensive understanding of regional patterns in LWD discharge dynamics and support the development of region-specific hazard mitigation strategies.

7. ACKNOWLEDGMENTS

The authors would like to thank the Water Resources Environment Technology Centre and the Japanese Ministry of Land, Infrastructure and Transport (MLIT) for their assistance in providing and collecting data on LW. The authors also thank Seiki Kawagoe, Katsuhiro Nakao, and Haruka Tsunetaka for their valuable advice. This research was funded by the Ministry of Land, Infrastructure, Transport and Tourism (MLIT), according to the 'Improving the reproducibility of large wood dynamics analysis using the integrated large wood export model (PI: Daisuke Komori)' and the Grants in Aid for Fostering Joint International Research (19KK0362, PI: Daisuke Komori) from the Ministry of Education, Science and Culture, Japan.

8. REFERENCES

1. Rengers F.K., McGuire L.A., Barnhart K.R., Youberg A.M., Cadol D., Gorr A.N., Kean J.W., The influence of large woody debris on post-wildfire debris flow sediment storage, Natural Hazards and Earth System Sciences, Vol. 23, No. 6, 2023, pp. 2075-2088. https://doi.org/10.5194/nhess-23-2075-2023
2. Schmocker L., Weitbrecht V., Driftwood: Risk analysis and engineering measures, Journal of Hydraulic Engineering, Vol. 139, No. 7, 2013, pp. 683-695. https://doi.org/10.1061/(ASCE)HY.1943-7900.0000728
3. Harmon M.E., Franklin J.F., Swanson F.J., Sollins P., Gregory S.V., Lattin J.D., Cummins K.W., Ecology of coarse woody debris in temperate ecosystems, Advances in Ecological Research, Vol. 15, 1986, pp. 133-302. https://doi.org/10.1016/S0065-2504(08)60121-X
4. Gurnell A.M., Piégay H., Swanson F.J., Gregory S.V., Large wood and fluvial processes, Freshwater Biology, Vol. 47, No. 4, 2002, pp. 601-619. https://doi.org/10.1046/j.1365-2427.2002.00916.x
5. Lucía, A., Comiti, F., Borga, M., Cavalli, M., & Marchi, L. (2015). Dynamics of large wood during a flash flood in two mountain catchments. Natural Hazards and Earth System Sciences, 15(8), 1741-1755. https://doi.org/10.5194/nhess-15-1741-2015
6. Lucía A., Comiti F., Borga M., Cavalli M., Marchi L., Dynamics of large wood during a flash flood in two mountain catchments, Natural Hazards and Earth System Sciences, Vol. 15, No. 8, 2015, pp. 1741-1755. https://doi.org/10.5194/nhess-15-1741-2015
7. Yumuang S., 2001 debris flow and debris flood in Nam Ko area, Phetchabun province, central Thailand, Environmental Geology, Vol. 51, No. 4, 2006, pp. 545-564. https://doi.org/10.1007/s00254-006-0351-9
8. Chaithong T., Komori D., Sukegawa Y., Touge Y., Mitobe Y., Anzai S., Landslides and precipitation characteristics during the Typhoon Lionrock in Iwate Prefecture, Japan, GEOMATE Journal, Vol. 14, No. 44, 2018, pp. 109-114. https://doi.org/10.21660/2018.44.7132
9. Kazama M., Yamakawa Y., Yamaguchi A., Yamada S., Kamura A., Hino T., Moriguchi S., Disaster report on geotechnical damage in Miyagi Prefecture, Japan caused by Typhoon Hagibis in 2019, Soils and Foundations, Vol. 61, No. 2, 2021, pp. 549-565. https://doi.org/10.1016/j.sandf.2020.12.001
10. Abe Y., Phakdimek S., Komori D., The relationship between large wood export and the long-term large wood budget on an annual scale in Japan, using storage function with the lumped hydrological method, Water, Vol. 16, No. 7, 2024, pp. 920. https://doi.org/10.3390/w16070920
11. Komori D., Sukegawa Y., Chaithong T., Kazama S., Modelling of large wood export at a watershed scale, Earth Surface Processes and Landforms, Vol. 47, No. 2, 2022, pp. 688-696. https://doi.org/10.1002/esp.5282
12. Seo J.I., Nakamura F., Chun K.W., Kim S.W., Grant G.E., Precipitation patterns control the distribution and export of large wood at the catchment scale, Hydrological Processes, Vol. 29, No. 24, 2015, pp. 5044-5057. https://doi.org/10.1002/hyp.10473
13. Yano S., Shogaki T., Yato S., Tsusue A., Wu Y., Kasama K., Development of logistic regression model for slope failure and estimation of driftwoods generation in Marumori Town due to the East Japan Typhoon 2019 [in Japanese with English abstract], Journal of Japan Society of Civil Engineers, Ser. B1 (Hydraulic Engineering), Vol. 76, No. 1, 2020, pp. 253-263. https://doi.org/10.2208/jscejhe.76.1_253
14. Kobayashi C., Shogaki T., Yato S., Wu Y., Fukuda R., Tsusue A., Maruya Y., Yano S., Field survey of driftwoods generation in the Kuma River and the Chikugo River due to the heavy rain in July 2020 and evaluation of driftwood disaster risk in the Kawabe River [in Japanese with English abstract], Journal of Japan Society of Civil Engineers, Ser. B1 (Hydraulic Engineering), Vol. 77, No. 1, 2021, pp. 174-184. https://doi.org/10.2208/jscejhe.77.1_174
15. Benda L.E., Sias J.C., A quantitative framework for evaluating the mass balance of in-stream organic debris, Forest Ecology and Management, Vol. 172, No. 1, 2003, pp. 1-16. https://doi.org/10.1016/S0378-1127(01)00576-X
16. Hassan M.A., Bird S., Reid D., Hogan D., Simulated wood budgets in two mountain streams, Geomorphology, Vol. 259, 2016, pp. 119-133. https://doi.org/10.1016/j.geomorph.2016.02.010
17. Nash J.E., Sutcliffe J.V., River flow forecasting through conceptual models Part I—A discussion of principles, Journal of Hydrology, Vol. 10, No. 3, 1970, pp. 282-290. https://doi.org/10.1016/0022-1694(70)90255-6